ChemComm

ROYAL SOCIETY OF CHEMISTRY

COMMUNICATION

View Article Online
View Journal | View Issue

Check for updates

Cite this: *Chem. Commun.*, 2023, **59**, 7815

Received 21st April 2023,
Accepted 29th May 2023

DOI: 10.1039/d3cc01949g

rsc.li/chemcomm

Published on 29 May 2023. Downloaded by NANJING UNIVERSITY on 6/21/2023 3:35:16 AM.

In situ evaluation of *in vivo* sialylation with a dual-color imaging strategy†

Shiya Zhao,‡ Yuanjiao Yang,‡ Yuru Wang, Huipu Liu, Huangxian Ju * and Yunlong Chen *

This work designs a functional dendrimer probe to conveniently identify newly generated sialic acid groups *in vivo* with a dual-color imaging strategy, which achieves *in situ* semiquantitative evaluation of the sialylation difference between tumor and normal tissues to reveal sialylation-related biological events and promote clinical tumor diagnosis.

Sialylation is an important glycosylation process,[1] which can introduce sialic acid (SA) to the outmost end of glycan chains attached on proteins, lipids, or RNAs.[2–4] As the terminal group of glycan, SA is the main executor of glycan functions,[5] and further mediates various physiological and pathological processes,[6,7] especially the migration,[8,9] metastasis[10,11] and immune evasion of tumor cells.[12,13] Thus, *in situ* evaluation of *in vivo* sialylation can promote more precise identification of SA-related biological processes. Although the goal of the direct detection of SA has been achieved by many methods,[14,15] methods for *in situ* evaluation of *in vivo* sialylation are still rare, which is an urgent demand to elucidate sialylation-related biological mechanisms for diagnostic and therapeutic applications.

To evaluate the sialylation, the signal response between the substrate and SA is the key issue. Generally, methods for direct detection of SA are essential to compose sialylation evaluation strategies, which usually utilize lectins,[16,17] chemical selectivity[18,19] or metabolic labeling[20,21] technologies to recognize SA. By introducing another signal label on the substrate, fluorescence resonance energy transfer (FRET) is an efficient tool for the construction of an intracellular glycosylation signal response. Some FRET based methods have been successfully used for *in situ* imaging of O-GlcNAcylation.[22,23] Our group has also achieved *in situ* evaluation and diversion of sialylation by FRET[24] and on-quencher fluorescent dyes.[25] However, these FRET based methods suffer from low signal sensitivity and high background. Besides, they need complex construction of the probes with engineered proteins or nanoparticles, which limits their applications *in vivo* and clinical applications.

Herein, this work developed a dual-color imaging strategy to *in situ* evaluate *in vivo* sialylation with a functional dendrimer probe. The dendrimer probe was conveniently constructed on a bis-MPA-acetylene dendrimer (Den-Acet), which was conjugated with azide-labeled galactose (Gal), folic acid (FA) and Cy5 groups through the click reaction[26–28] and amide condensation (Fig. 1A).[29] In the obtained Den-Gal/Cy5/FA probe, Gal is the substrate for the sialylation proceeding by α-2,3-sialyltransferase (ST3Gal) and α-2,6-sialyltransferase (ST6Gal),[30,31] and FA was used for receptor-mediated endocytosis of the probes into tumor cells.[32,33] By injecting the probes into the tumor region in a living mouse, SA groups were bound to the Gals on Den-Gal/Cy5/FA through sialylation (Fig. 1B). After collection and sectioning of the tumor tissue, the tissue slices were sequentially treated with sodium periodate ($NaIO_4$) and fluorescein-5-thiosemicarbazide (FTZ) to label the SA with FTZ fluorescence.[19,34] Restricted by the nanoscale size of the

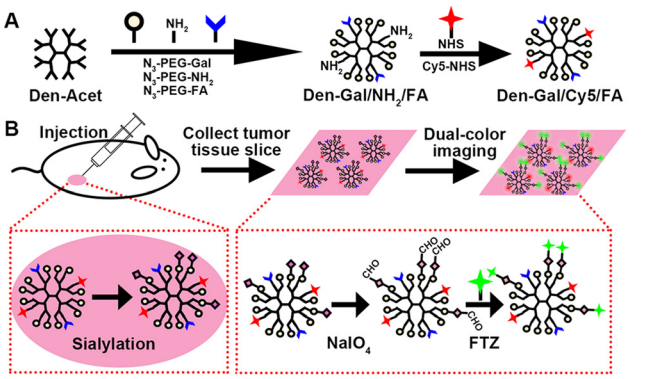

Fig. 1 Schematic illustration. (A) Preparation of the dendrimer probe Den-Gal/Cy5/FA. (B) *In situ* evaluation of *in vivo* sialylation by dual-color imaging.

State Key Laboratory of Analytical Chemistry for Life Science, School of Chemistry and Chemical Engineering, Nanjing University, Nanjing 210023, China. E-mail: hxju@nju.edu.cn, ylc@nju.edu.cn

† Electronic supplementary information (ESI) available. See DOI: https://doi.org/10.1039/d3cc01949g

‡ These authors contributed equally to this work.

Published on 29 May 2023. Downloaded by NANJING UNIVERSITY on 6/21/2023 3:35:16 AM.

Den-Gal/Cy5/FA, the FTZ fluorescence overlying the Cy5 fluorescence was used to identify the newly generated SA, which could be used for evaluation of the sialylation difference between tumor and normal tissues. This work provides a convenient tool for *in situ* evaluation of *in vivo* sialylation, which exhibits huge potential for revealing sialylation-related biological events and clinical tumor diagnosis.

For the preparation of the functional dendrimer probe, the generation 5 bis-MPA-acetylene dendrimer was chosen as the substrate, which contains 96 acetylene groups for efficient modification of the functional groups. As the substrate for sialylation, N_3-PEG-Gal was prepared by deacetylation of N_3-PEG-Gal-4Ac using esterase (Fig. S1A, ESI†).[35] The ESI-MS analysis demonstrated the successful deacetylation of N_3-PEG-Gal-4Ac (Fig. S1B, m.w. 528, + Na^+, ESI†) to obtain N_3-PEG-Gal (Fig. S1C, m.w. 360, + Na^+, ESI†). The Den-Acet was firstly covalently bound with N_3-PEG-Gal, N_3-PEG-NH_2, and N_3-PEG-FA through Cu-BTTAA catalyzed click reaction. The obtained Den-Gal/NH_2/FA was then conjugated with NHS-Cy5 to obtain Den-Gal/Cy5/FA through the amide condensation between the NH_2 and NHS groups. The nanoscale sizes of Den-Acet and Den-Gal/Cy5/FA were firstly characterized by transmission electron microscopic (TEM) and dynamic light scattering (DLS) analysis (Fig. S2, ESI†), which exhibited narrow size distributions of hydrodynamic diameters around 10 and 13 nm. The successful conjugation of Cy5 was obviously observed by the color change of the dendrimer probes from light yellow (Fig. S3A, tube 1, ESI†) to deep blue (Fig. S3A, tube 2, ESI†) after Cy5 conjugation. In contrast, the production of Den-Gal/FA with NHS-Cy5 appeared light blue (Fig. S3A, tube 3, ESI†). Meanwhile, the fluorescence spectra of Den-Gal/Cy5/FA exhibited strong Cy5 fluorescence, while that of the production of Den-Gal/FA with NHS-Cy5 and Den-Gal/NH_2/FA was weak (Fig. S3B and C, ESI†). Thus, the Cy5 groups were successfully covalently conjugated to the dendrimer using N_3-PEG-NH_2 as the linker with negligible nonspecific adsorption.

The successful modification of FA was demonstrated by infrared spectra (Fig. S4, ESI†), which exhibited extra characteristic absorption peaks of N_3-PEG-FA around 2350 cm^{-1} in Den-Gal/Cy5/FA compared to that of Den-Gal/Cy5. To verify the successful conjugation of Gal to the dendrimer probe, a FITC-SBA lectin chip was prepared, which could specifically recognize Gal.[36] The FITC fluorescence intensity on the initial SBA lectin chip suggested a uniform decoration of each lectin spot on the chip (Fig. S5A and B, ESI†). After incubation with Den-Gal/Cy5/FA (Fig. S5C line 1, ESI†), Den-Gal/Cy5 (Fig. S5C line 2, ESI†) and Den-Cy5/FA (Fig. S5C line 3, ESI†), both Den-Gal/Cy5/FA and Den-Gal/Cy5 exhibited similarly strong Cy5 fluorescence on the lectin spots, while that of Den-Cy5/FA exhibited tiny nonspecific adsorption (Fig. S5D, ESI†). Thus, the successful conjugation of Gal on the dendrimer probe was effectively demonstrated.

The N_3-PEG-Gal in this work contains two reactive hydroxyl groups at both positions 3 and 6 of the sugar ring,[37] which are the acceptor sites of ST3Gal and ST6Gal. To investigate the *in vitro* performance of Den-Gal/Cy5/FA for these STs, a FITC-SNA lectin chip was prepared, which could specifically recognize SA[38] on the sialylated Den-Gal/Cy5/FA. Den-Gal/Cy5/FA was incubated with CMP-Sia and ST3Gal or ST6Gal in PBS (pH 7.4) at 37 °C for 2 h, respectively. 100 nM of the products was directly dropped onto the different spots on the SNA lectin chip. The FITC fluorescence intensity on the initial SNA lectin chip suggested a uniform decoration of each lectin spot on the chip (Fig. 2A and B). After incubation with 100 nM of Den-Gal/Cy5/FA and the formation of different products, both the products of Den-Gal/Cy5/FA with ST3Gal (Fig. 2C and D line 2) and Den-Gal/Cy5/FA with ST6Gal (Fig. 2C and D line 3) exhibited strong Cy5 fluorescence on the lectin spot, while that of raw Den-Gal/Cy5/FA exhibited tiny nonspecific adsorption (Fig. 2C and D line 1). Thus, the Den-Gal/Cy5/FA could be successfully sialylated by ST3Gal and ST6Gal *in vitro*, which could also be an efficient substrate for *in vivo* applications.

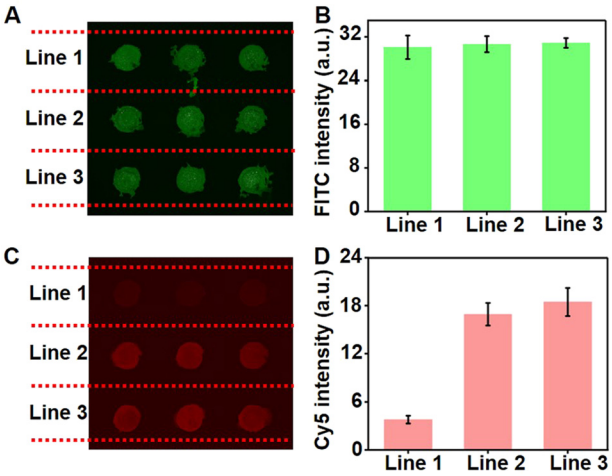

Fig. 2 (A) Fluorescence images of the initial SNA lectin chip. Lines 1–3 were the same. (B) Average FITC fluorescence intensities from (A). (C) Fluorescence images of the SNA lectin chip incubated with Den-Gal/Cy5/FA (line 1), and products of Den-Gal/Cy5/FA with ST3Gal (line 2) and Den-Gal/Cy5/FA with ST6Gal (line 3). (D) Average Cy5 fluorescence intensities from (C). Error bars represent ± S.D. (n = 3).

As a proof-of-concept, mouse breast cancer 4T1 cells were chosen as the cell model. Normal mammary epithelial MCF-10A cells were used as a negative control. The optimized time for the probe entry was proved to be 60 min by confocal laser scanning microscope (CLSM) images of cells treated with Den-Gal/Cy5/FA for regular time intervals (Fig. S6, ESI†). 4T1 and MCF-10A cells were incubated with different concentrations of Den-Gal/Cy5/FA or Den-Cy5/FA (10–250 nM) at 37 °C for 1 h. After the cells were washed and fixed, the SA groups were oxidized by $NaIO_4$, and were further labeled with FTZ through aniline catalysis. The CLSM images showed obvious FTZ (green) and Cy5 (red) fluorescence distributed inside 4T1 cells, but weak FTZ fluorescence inside MCF-10A cells (Fig. S7, ESI†). Here, the FTZ fluorescence indicated the distribution of both the original and newly generated SA groups, and the Cy5 fluorescence indicated the distribution of Den-Gal/Cy5/FA or Den-Cy5/FA probes. Through the colocalization of FTZ fluorescence with Cy5 fluorescence, the FTZ@Cy5 fluorescence images were obtained by

 This journal is © The Royal Society of Chemistry 2023

Published on 29 May 2023. Downloaded by NANJING UNIVERSITY on 6/21/2023 3:35:16 AM.

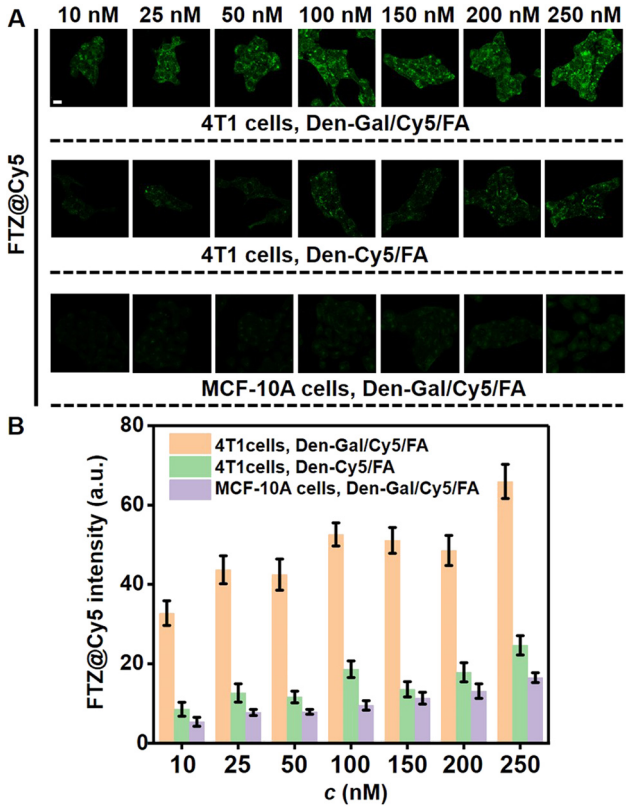

Fig. 3 (A) Colocalization of FTZ fluorescence with Cy5 fluorescence obtained by collecting the FTZ fluorescence within the Cy5 fluorescence area in Fig. S7 (ESI†). Scale bar: 20 μm. (B) Statistical FTZ@Cy5 intensities from (A). Error bars represent ± S.D. (n = 3).

collecting the FTZ fluorescence within the Cy5 fluorescence area (Fig. 3). Considering that the newly generated SA groups mainly occurred on Den-Gal/Cy5/FA probes restricted within a nanoscale space, the FTZ@Cy5 fluorescence images could correctly identify the existence of newly generated SA groups. As a result, the 4T1 cells treated with Den-Gal/Cy5/FA exhibited obvious FTZ@Cy5 signals (Fig. 3), which increased with increased probe concentrations. In contrast, the 4T1 cells treated with Den-Cy5/FA only exhibited weak FTZ@Cy5 signals after the probe concentration was higher than 200 nM. Besides, the MCF-10A cells treated with Den-Gal/Cy5/FA constantly exhibited tiny FTZ@Cy5 signals with the increased probe concentrations, which was consistent with the low SA expression in normal cells.[39] Thus, through an accurate regulation of the probe concentration, the Den-Gal/Cy5/FA could provide a high specificity to visualize the newly generated SA inside cells.

As an alternate way to detect SA inside cells, FITC-SNA was applied to recognize SAs instead of $NaIO_4$ oxidation and FTZ labeling. As a result, strong FITC fluorescence was observed on the 4T1 cell surface (Fig. S8, ESI†), and the colocalized FITC@Cy5 signals exhibited poor signal to background ratio between Den-Gal/Cy5/FA and Den-Cy5/FA treated cells (Fig. S9, ESI†). This may be attributed to the big FITC-SNA size, which hindered its entrance into cells. Thus, the $NaIO_4$ oxidation and FTZ labeling route exhibited an advantage for intracellular labeling, which further promised its application *in vivo*.

For the preliminary *in vivo* application of the designed strategy, the 4T1 tumor xenograft mice models were established by subcutaneous inoculation of 4T1 cells in the selected position of the mice. To investigate the retention of the dendrimer probes *in vivo*, Den-Gal/Cy5/FA was subcutaneously injected into the tumor region. The fluorescence images of the mouse exhibited obvious Cy5 fluorescence at the tumor region, which exhibited a persistent retention within 60 min and was excreted from the tumor region after 150 min (Fig. S10, ESI†). Therefore, the tumor tissue slices were prepared after 1 h of injection with a standard procedure. After DAPI staining of the cell nucleus, the obtained slices were subjected to $NaIO_4$ oxidation and FTZ labeling, and were finally subjected to CLSM imaging. Through the colocalization of FTZ fluorescence with Cy5 fluorescence, the fluorescence images of the tumor tissue slices from the Den-Gal/Cy5/FA treated mice exhibited obvious FTZ@Cy5 signal, while that of the Den-Cy5/FA treated mice only exhibited weak background signal (Fig. S11, ESI†), which demonstrated the feasibility of the designed dual-color imaging strategy in *in vivo* applications.

To explore the difference of sialylation between tumor tissue and normal tissue, the Den-Gal/Cy5/FA was subcutaneously injected into the tumor region and normal tissue at the symmetrical position of the mouse simultaneously. After the same slice preparation and dual-color imaging strategy, the FTZ@Cy5 signal of the tumor tissue was 2.5 times stronger than that of the normal tissue (Fig. 4). After eliminating the certain background signal of the dendrimer probes (Fig. S11, ESI†), the sialylation level in the tumor tissue should be around two times higher than that of normal tissue. Thus, the designed dual-color strategy achieved semiquantitative evaluation of the sialylation *in vivo*.

In the *in vivo* applications, the replacement of the $NaIO_4$ oxidation and FTZ labeling route with FITC-SNA was also tested. Unsurprisingly, the FITC@Cy5 signals exhibited a strong background signal in the tumor tissue from the Den-Cy5/FA treated mouse (Fig. S12, ESI†), and gave an inefficient discrimination between tumor and normal tissues (Fig. S13, ESI†), which further demonstrated the advantage of the $NaIO_4$ oxidation and FTZ labeling route in the designed dual-color strategy.

In conclusion, a dual-color imaging strategy was designed for *in situ* evaluation of *in vivo* sialylation in tumor xenografted mice. This strategy utilizes Den-Gal/Cy5/FA as the substrate to introduce newly generated SA groups, which can be efficiently labeled with the $NaIO_4$ oxidation and FTZ labeling route. Through the colocalization of FTZ fluorescence with Cy5 fluorescence restricted within a nanoscale space, the newly generated SA groups can be conveniently identified for the semiquantitative evaluation of the sialylation *in vivo*. By use of other substrates and labeling routes, this strategy can be expanded for the evaluation of different biological modification pathways, which provides a convenient and extensible tool for revealing posttranslational modification-related biological mechanisms and clinical tumor diagnosis.

Published on 29 May 2023. Downloaded by NANJING UNIVERSITY on 6/21/2023 3:35:16 AM.

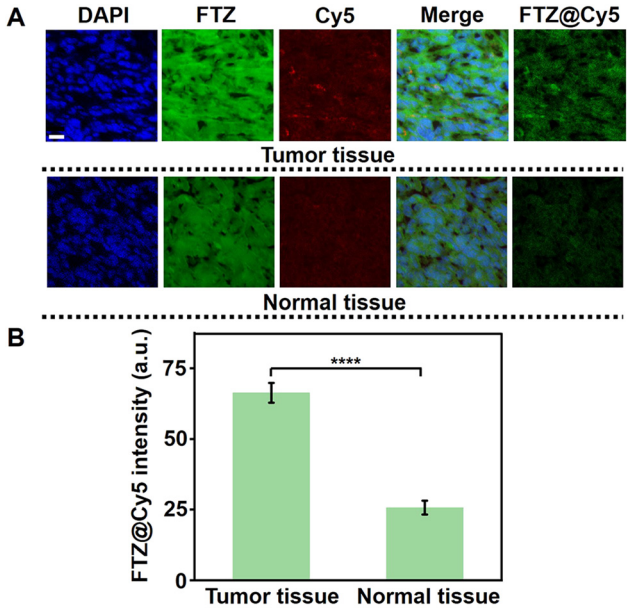

Fig. 4 (A) CLSM images of the tumor and normal tissue slices from a Den-Gal/Cy5/FA treated mouse after DAPI staining, $NaIO_4$ oxidation and FTZ labeling. Scale bar: 20 μm. (B) Statistical FTZ@Cy5 intensities from (A). Error bars represent ± S.D. (n = 3). Statistical significance is determined by unpaired two-tailed Student's t-test (*$P < 0.05$; **$P < 0.01$; ***$P < 0.001$; ****$P < 0.0001$).

This work was supported by the National Natural Science Foundation of China (21974063, 21827812, and 21890741). This study was performed in strict accordance with the Laboratory Animal Management of Jiangsu Province for the care and use of laboratory animals (License no. SYXK 2019-0056) and was approved by the Department of Science and Technology of Jiangsu Province (Nanjing, China).

Conflicts of interest

There are no conflicts to declare.

Notes and references

1 A. Varki, R. L. Schnaar and R. Schauer, *Essentials of glycobiology*, Cold Spring Harbor Laboratory Press, New York, 2015.
2 W. R. Alley Jr and M. V. J. Novotny, *Proteome Res.*, 2010, **9**, 3062–3072.
3 M. M. Fuster and J. D. Esko, *Nat. Rev. Cancer*, 2005, **5**, 526–542.
4 R. A. Flynn, K. Pedram, S. A. Malaker, P. J. Batista, B. A. H. Smith, A. G. Johnson, B. M. George, K. Majzoub, P. W. Villalta, J. E. Carette and C. R. Bertozzi, *Cell*, 2021, **184**, 3109–3124.
5 A. L. Lewis, N. Desa, E. E. Hansen, Y. A. Knirel, J. I. Gordon, P. Gagneux, V. Nizet and A. Varki, *Proc. Natl. Acad. Sci. U. S. A.*, 2009, **106**, 13552–13557.
6 A. Varki, *Nature*, 2007, **446**, 1023–1029.
7 X. Chen and A. Varki, *ACS Chem. Biol.*, 2010, **5**, 163–176.
8 A. Matsumoto, H. Cabral, N. Sato, K. Kataoka and Y. Miyahara, *Angew. Chem., Int. Ed.*, 2010, **49**, 5494–5497.
9 A. Varki, *Trends Mol. Med.*, 2008, **14**, 351–360.
10 D. H. Dube and C. R. Bertozzi, *Nat. Rev. Drug Discovery*, 2005, **4**, 477–488.
11 Y. F. Xu, A. Sette, J. Sidney, S. J. Gendler and A. Franco, *Immunol. Cell Biol.*, 2005, **83**, 440–448.
12 J. E. Hudak, S. M. Canham and C. R. Bertozzi, *Nat. Chem. Biol.*, 2014, **10**, 69–75.
13 H. Läubli, O. M. T. Pearce, F. Schwarz, S. S. Siddiqui, L. Deng, M. A. Stanczak, L. Deng, A. Verhagen, P. Secrest, C. Lusk, A. G. Schwartz, N. M. Varki, J. D. Bui and A. Varki, *Proc. Natl. Acad. Sci. U. S. A.*, 2014, **111**, 14211–14216.
14 Y. L. Chen, L. Ding and H. X. Ju, *Chem. Commun.*, 2013, **49**, 862.
15 W. Y. Song, L. Ding, Y. L. Chen and H. X. Ju, *Chem. Commun.*, 2016, **52**, 10640.
16 H. Lis and N. Sharon, *Chem. Rev.*, 1998, **98**, 637–674.
17 W. I. Weis and K. Drickamer, *Annu. Rev. Biochem.*, 1996, **65**, 441–473.
18 J. Nilsson, U. Ruetschi, A. Halim, C. Hesse, E. Carlsohn, G. Brinkmalm and G. Larson, *Nat. Methods*, 2009, **6**, 809–811.
19 Y. Zeng, T. N. C. Ramya, A. Dirksen, P. E. Dawson and J. C. Paulson, *Nat. Methods*, 2009, **6**, 207–209.
20 S. T. Laughlin and C. R. Bertozzi, *Nat. Protoc.*, 2007, **2**, 2930–2944.
21 J. A. Prescher and C. R. Bertozzi, *Cell*, 2006, **126**, 851–854.
22 W. Lin, L. Gao and X. Chen, *ChemBioChem*, 2015, **16**, 2571–2575.
23 F. Doll, A. Buntz, A.-K. Späte, V. F. Schart, A. Timper, W. Schrimpf, C. R. Hauck, A. Zumbusch and V. Wittmann, *Angew. Chem., Int. Ed.*, 2016, **55**, 2262–2266.
24 L. Bao, L. Ding, M. Yang and H.-X. Ju, *Sci. Rep.*, 2015, **5**, 10947.
25 Y. L. Chen, H. P. Liu, L. Ding and H. X. Ju, *Anal. Chem.*, 2018, **90**, 3073–3078.
26 H. C. Kolb, M. Finn and K. B. Sharpless, *Angew. Chem., Int. Ed.*, 2001, **40**, 2004–2021.
27 M. Meldal and C. W. Tornøe, *Chem. Rev.*, 2008, **108**, 2952–3015.
28 C. J. Hawker and K. L. Wooley, *Science*, 2005, **309**, 1200.
29 G. T. Hermanson, *Bioconjugate Techniques*, Academic Press, 2008.
30 P. D. Bos, X. H.-F. Zhang, C. Nadal, W. Shu, R. R. Gomis, D. X. Nguyen, A. J. Minn, M. J. van de Vijver, W. L. Gerald, J. A. Foekens and J. Massagué, *Nature*, 2009, **459**, 1005–1009.
31 A. Harduin-Lepers, M.-A. Krzewinski-Recchi, F. Colomb, F. Foulquier, S. Groux-Degroote and P. Delannoy, *Front. Biosci.*, 2012, **4E**, 499–515.
32 A. Cheung, H. J. Bax, D. H. Josephs, K. M. Ilieva, G. Pellizzari, J. Opzoomer, J. Bloomfield, M. Fittall, A. Grigoriadis, M. Figini, S. Canevari, J. F. Spicer, A. N. Tutt and S. N. Karagiannis, *Oncotarget*, 2016, **7**, 52553–52574.
33 R. Ghiarasim, N. Simionescu, A. Coroaba, C. M. Uritu, N. L. Marangoci, S.-A. Ibanescu and M. Pinteala, *Int. J. Mol. Sci.*, 2022, **23**, 155.
34 P. W. Zhang, Y. R. Li, X. F. Yu, H. X. Ju and L. Ding, *Chem. – Eur. J.*, 2019, **25**, 10505–10510.
35 A. Baba and T. Yoshioka, *Org. Biomol. Chem.*, 2006, **4**, 3303–3310.
36 H. Lis, B. A. Sela, L. Sachs and N. Sharon, *Biochim. Biophys. Acta*, 1970, **211**, 582–585.
37 Y. L. Chen, Y. J. Yang, Q. Q. Tan, H. P. Liu and H. X. Ju, *Chem. Sci.*, 2022, **13**, 2939.
38 N. Shibuya, I. J. Goldstein, W. F. Broekaert, M. Nsimba-Lubaki, B. Peeters and W. J. J. Peumans, *Biol. Chem.*, 1987, **262**, 1596–1601.
39 X. Ma, W. Dong, Z. Su, L. Zhao, Y. Miao, N. Li, H. Zhou and L. Jia, *Cell Death Dis.*, 2016, **7**, e2561.

 This journal is © The Royal Society of Chemistry 2023